Bioengineering

https://www.aimspress.com/journal/Bioengineering

AIMS Bioengineering, 12(3): 370–382.
DOI: 10.3934/bioeng.2025017
Received: 05 June 2025
Revised: 29 June 2025
Accepted: 18 July 2025
Published: 22 July 2025

Research article

sEMG-based lower-limbs motion recognition using deep learning with one dimensional convolutional neural network

Li Zhang[1,2,3], Hui Li[2], Qingqi Zhu[4], Xiaobo Zhang[5], Hongbin Zhang[4], Heng Zhang[4], Chao Lu[2,*], Peng Xu[2], Aibin Zhu[6] and Pingping Wei[7]

[1] Xi'an Jiaotong University, Xi'an, 710049, China
[2] Honghui Hospital, Xi'an Jiaotong University, Xi'an, 710054, China
[3] Xi'an Key Laboratory of Pathogenesis and Precision Treatment of Arthritis, Xi'an, 710054, China
[4] School of Mechanical Engineering, Northwestern Polytechnical University, Xi'an, 710072, China
[5] School of Mechanical Engineering, Xijing University, Xi'an, 710123, China
[6] Shaanxi Key Laboratory of Intelligent Robots, Institute of Robotics and Intelligent Systems, Xi'an Jiaotong University, Xi'an, 710049, China
[7] State Key Laboratory for Manufacturing Systems Engineering, Xi'an Jiaotong University, Xi'an, 710054, China

* **Correspondence:** Email: luchao0925@163.com.

Abstract: Surface electromyographic (sEMG)-based motion recognition has been successfully applied in the exoskeleton, human–machine interaction, and rehabilitation engineering. To improve the accuracy of motion recognition and then achieve accurate control of the exoskeleton, this paper is devoted to proposing a one-dimensional (1D) convolutional neural network (1D-CNN) to classify seven daily lower-limb motions from the eight main muscles of human lower limbs. The proposed model architecture mainly consisted of three 1D convolutional layers, three max-pooling layers, and one global average pooling layer. The Teager–Kaiser energy operator was adopted for the starting and ending points detection of sEMG signals. To avoid overfitting, only two features (i.e., mean absolute value (MAV) and root mean square (RMS)) were extracted in this study and used as the input of the proposed model. The results show that the accuracy of motion recognition based on our proposed model had been improved to more than 97.0 ± 0.8% and was higher than that based on the deep neural network (DNN) and support vector machine (SVM) models (95.0 ± 0.6% and 92.8 ± 0.7%). The research results and proposed model of this study are significant for research into exoskeleton control based on sEMG signals.

Keywords: surface electromyography; one dimensional convolutinal neural network; motion recognition; lower limb; exoskeleton

1. Introduction

Surface electromyographic (sEMG)-based human motion recognition has been successfully applied in the exoskeleton, human–machine interaction, and rehabilitation engineering [1–3]. sEMG signals, which contains a lot of information about muscle movement, are a type of physiological signal caused by human muscle activity. Since sEMG is a predictor of motion patterns, a common use of sEMG signals is to convert the signal into a control signal for an executable command of a device e.g., prosthesis or exoskeleton [2]. To control the exoskeleton more accurately, the classification algorithm, which is also known as the classifier, is commonly used to recognize human motion patterns and in control strategies [4].

Currently, several different classifiers have been developed to recognize human motion patterns. Zhang et al. [5] established a back-propagation neural network (BPNN) based on the arm sEMG signals from seven muscles to discriminate seven classes of arm motions. Asai et al. [6] utilized a convolutional neural network (CNN) model based on frequency conversion of sEMG signals to estimate four finger motions, including thumb close, thumb open, fingers except thumb close, and fingers except thumb open. Crepin et al. [7] classified 13 hand motions on the basis of forearm sEMG singles from seven channels using a linear discriminant analysis (LDA) approach. Zhao et al. [8] proposed a model based on sEMG signals, which combined convolutional neural networks, bidirectional long short-term memory (LSTM) networks, and an attention mechanism, to classify five upper limb motions, including static loading-bearing, dynamic load-bearing, mild activity, rapid movement, and resting. Zhou et al. [9] established a CNN–Transformer–LSTM (CNN-TL) fusion model based on the lower limb sEMG signals from seven muscles to classify four lower limb motions, including walking, ascending stairs, descending stairs, and squatting. Shi et al. [10] proposed a scale unscented Kalman neural network based on sEMG signals from three lower limb muscles to classify five motions, including walking, crossing obstacles, standing up, ascending stairs, and descending stairs. In general, most of the current studies focus on the recognition of upper limb motions, while there are relatively fewer studies on the recognition of lower limb motions. For lower limb motion recognition, the recognition accuracy of current studies is relatively low and the types of recognized motions of current studies are relatively limited.

The sEMG signal is the input of the classifier, which can learn very complex functions and then classify the motions. However, the raw sEMG signal contains a lot of useless signal noise. If the raw signal is used as the input of the classifier, the efficiency of classification will be reduced. The raw sEMG signal has to be preprocessed before being fed into the classifier. Common preprocessing processes of sEMG signals include signal filtering, starting and ending detection, and feature extraction. The frequency of the raw sEMG signal is 0–500 Hz. However, the available frequency of the sEMG signal is dominant between 50 and 150 Hz [11,12]. For signal filtering, band-pass filters, band-stop filters, and other filters are used to extract useful frequency bands from the raw sEMG signal. As a micro-electric signal, the signal-to-noise ratio (SNR) of the sEMG signal is relatively low. It is difficult to make an accurate judgment of the starting time and ending time of muscle movement. The Teager–Kaiser energy operator (TKEO) method, which amplifies the useful part of the signal while minimizing the noise, can be used in the detection of voice energy [13]. In recent years, it has been used for the detection of the starting and ending time of sEMG signals. The TKEO method can improve the SNR of the sEMG signal by emphasizing both the amplitude and frequency of motor-unit action potentials. Therefore, the accuracy of the starting and ending detection could be improved [14,15]. For feature extraction, the computational complexity, maximum class separability, and robustness must be considered [16]. The commonly used features include the time-domain and the frequency-domain features. For the time-domain features, there are several common features such as the mean absolute value (MAV), root mean square (RMS), and variance (VAR), among others [17–19]. For the frequency domain, the common features are the coefficients of the wavelet transform (WT) and the short-time Fourier transform (STFT) [20,21].

To improve the accuracy of motion recognition and then achieve accurate control of the exoskeleton, this paper is devoted to (1) proposing a one-dimensional (1D) convolutional neural network (1D-CNN) to classify daily lower limb motions from the main lower limb muscles; (2) adopting a Teager–Kaiser energy operator to improve the detection accuracy of the starting and ending points of the sEMG signals; and (3) improving the recognition accuracy of daily lower limb motions. We hypothesized that the proposed model could improve motion recognition accuracy compared with the commonly used deep neural network (DNN) algorithm and support vector machine (SVM).

2. Materials and methods

2.1. Subject and sEMG data acquisition

Three healthy men (age: 23 ± 1 years; mass: 67.7 ± 2.5 kg; and height: 176 ± 4 cm) were recruited in our study. The recruited subjects had no previous history of lower limb injuries or other neuromuscular disease. The study was approved by the Ethics Committee of Honghui Hospital, Xi'an Jiaotong University (Registration Number 202309006). Prior to the experiments, the subjects provided written informed consent.

A wireless sEMG acquisition system (Biovision, Germany) was utilized to capture the sEMG signal of the lower limbs. The data were sampled at a sampling rate of 1000 Hz. Eight electronics were attached to the eight main muscles of the subject's right lower limb (rectus femoris, vastus medial, vastus lateralis, biceps femoris, gastrocnemius medial, gastrocnemius lateralis, soleus, and tibialis anterior). Before the test, the subject's skin below the electronics was prepared by shaving off hair, exfoliated, and cleaned with an alcohol swab to improve the electronic–skin contact and minimize skin impedance.

Seven daily motions, namely walking forward, walking back, jogging, going upstairs, going downstairs, standing up, and sitting down, were selected in this study. For standing up and sitting down, 150 repetitions were utilized. To avoid muscle fatigue, the subject rested for 5 minutes every 15 trials. For walking forward, jogging, and walking back, the experiment was repeated 30 times on a 10-m walkway, with a 5-minute break every 10 trials. For going up and down stairs, the number of stairs was 12, and the exercise was repeated 30 times, with a 5-minute rest every 10 trials.

2.2. sEMG preprocessing

Once the data had been acquired, the sEMG time series were digitally filtered channel-wise. First, an 8th-order band-stop filter (50 Hz) was used to exclude the power line interference, and then an 8th-order band-pass filter (20–450 Hz) was used to suppress the noise and remove any DC offsets [11,16].

Since the TKEO method was adopted in this paper to detect the starting and ending points of the filtered signal, the sEMG signal was transformed into a TKEO signal first [22]. The discrete TKEO Ψ is calculated by:

$$\Psi[x(n)] = x^2(n) - x(n+1)x(n-1) \tag{1}$$

where n is the sample number and x is the signal. Then the mean values and variance of the 10-s baseline sEMG signal were calculated for each motion, and the threshold of onset detection could be obtained by:

$$T_i = \mu_i + h_i s_i\,, \quad i = 1, 2, \dots, 7 \tag{2}$$

where h is a preset variable, and μ and s are the mean values and variance, respectively.

Because the range of signal amplitude for each type of motion was different, the values of T_i were calculated separately by Eq. (2). After comparing the sEMG signal amplitude of eight lower limb muscles, the rectus femoris was the most active muscle during the seven motions. Therefore, the sEMG signals of rectus femoris were used to detect the beginning and ending points. After the sEMG signals of seven motions were intercepted, the datasets used for feature extraction could be obtained.

Due to the need for the Fourier transform, the relatively low real-time performance, and the relatively large computational resources, the frequency domain and the time-frequency domain features were not suitable for this study. Therefore, the time domain features, which were directly obtained from the time series of the sEMG signals, were used for feature extraction. To prevent overfitting and minimize computational resource consumption, the two commonly used time domain features, i.e., MAV and RMS, were extracted in this study.

$$\mathrm{MAV} = \frac{1}{N}\sum_{n=1}^{N}|x_n| \tag{3}$$

$$\mathrm{RMS} = \sqrt{\frac{1}{N}\sum_{n=1}^{N}(x_n)^2} \tag{4}$$

where x_n is the sEMG signal for each subwindow.

According to the study of [23], the calculation latency of real-time execution should be less than 300 ms to ensure fluidity of movement. Therefore, the time window of this study was set to 256 ms. As shown in Figure 1, in each 256-ms window, the overlapped subwindow with a 32-ms increment and a 128-ms length (overlap) was used to segment the window. The high overlap ratio (75%) was adopted to ensure the temporal continuity of the sEMG signals, prevent the loss of transient motion features, and achieve an optimal balance between computational efficiency and feature resolution. This aligns with previous studies, where a similar overlap ratio was used to ensure recognition accuracy [24,25]. The window slid five steps in the data to get five subwindows (128 × 1 vectors). In general, two times domain features were extracted from these five subwindows for eight channels (eight muscles) to obtain 80 features.

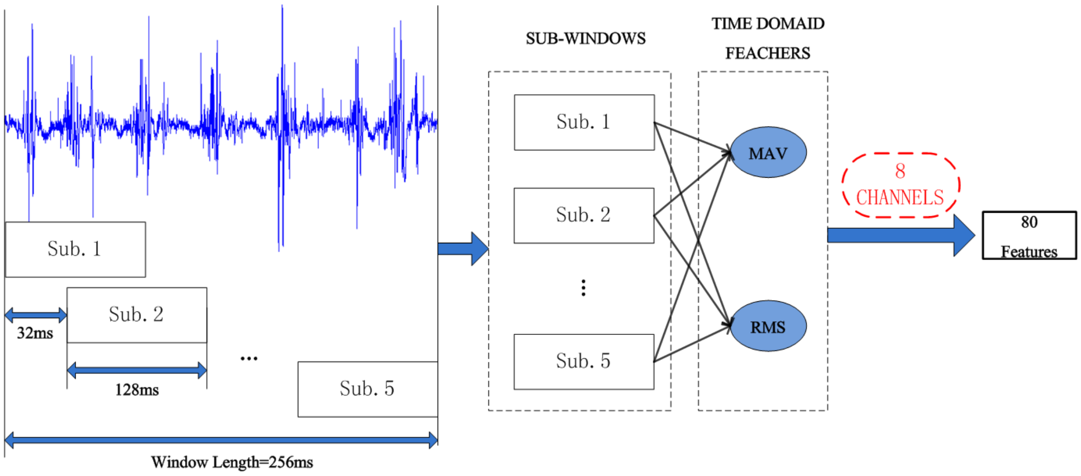

Figure 1. Feature extraction process.

2.3. Algorithm development

To improve the motion recognition accuracy, a 1D-CNN model was proposed in this study. As shown in Figure 2, a total of 80 features were fed into the 1D-CNN. In the model, there were three 1D convolutional layers, three max-pooling layers, and one global average pooling layer. Moreover, the width of all filter detectors was 10 × 1. The number of feature detectors in each convolutional layer was 64, 128, and 256, respectively. The feature detectors slid through the output data of the 1D convolutional layers and max-pooling layers with a stride of 1 and 2, respectively. In addition to the softmax activation function applied to the last layer (global average pooling layer), the rectified linear unit (ReLU) activation function was adopted to the output of each convolutional layer. These activation functions were used to help the network acquire nonlinear characteristics, while the pooling functions were reflected in the reduction in sampling: retaining significant characteristics, reducing feature dimensions, and increasing the receptive field of the detectors. The dropout technique was applied on all of the convolutional layers (dropout rate: 0.4). The global average pooling layer was applied as the last layer in our proposed algorithm. Compared with the traditional fully connected layer, this last layer could enhance the correspondence between feature mapping and category and avoid overfitting in this layer [26]. In the layer, a softmax activation function was used to calculate the probability for each class.

To compare the accuracy of lower-limb motion recognition, a DNN model and an SVM model were constructed. For the DNN, the model with five hidden layers was adopted (see Figure 3). The input layer accepted 80 features, and the last hidden layer ran a softmax activation function to output the probability of seven classes of movement. The node number of each hidden layer was 512, 256, 128, 64, and 32, respectively. For the output of each hidden layer, the ReLU activation function was adopted. The dropout technique was applied on all hidden layers (dropout rate: 0.4).

For the SVM, the kernel function (K) was set as the radial basis function (RBF) and can be calculated by:

$$K(x, x_i) = e^{-\frac{||x-x_i||}{2\sigma^2}} \tag{5}$$

where x_i is a support vector (SV). To make the SVM computationally very efficient, the number of SVs is considerably lower than the number of training samples in our study. The SVM included two parameters: C and γ. C reflects the penalty coefficient of the model to the error. The larger the C, the easier the model is to overfit. Here, γ is the coefficient of the kernel, which reflects the distribution of data mapping to higher-dimensional feature spaces. The larger the γ, the more the SVs, and vice versa. The grid search method was used to traverse the values of C and γ to find the optimal values. Eight values of C and γ were set from 1 to 100,000, increasing by a factor of 10. Then these values were paired with each other. Finally, it was found that the accuracy was highest when γ was 1 and C was 1000.

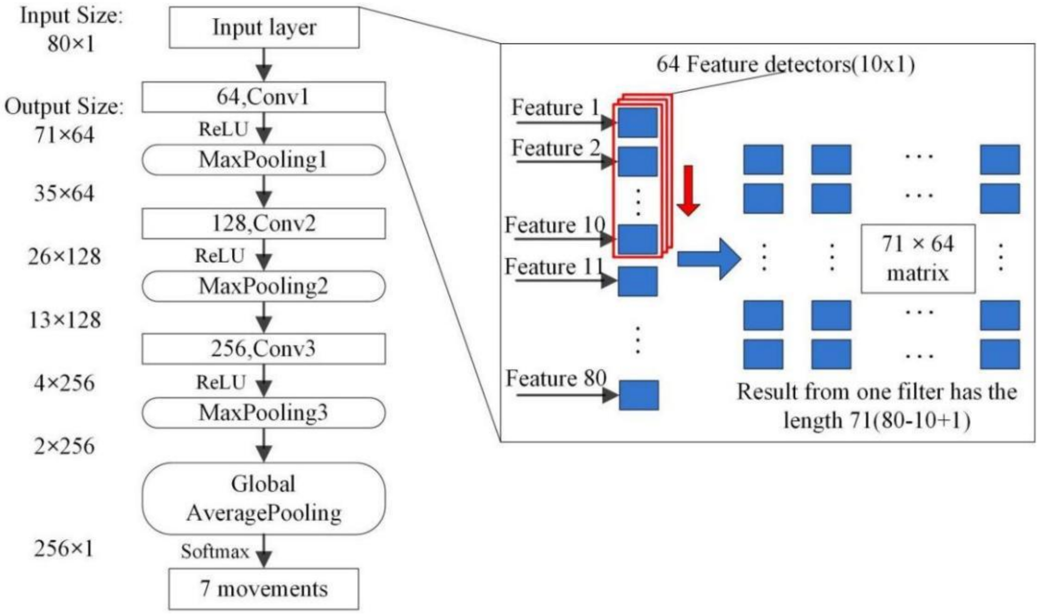

Figure 2. The architecture of the 1D-CNN.

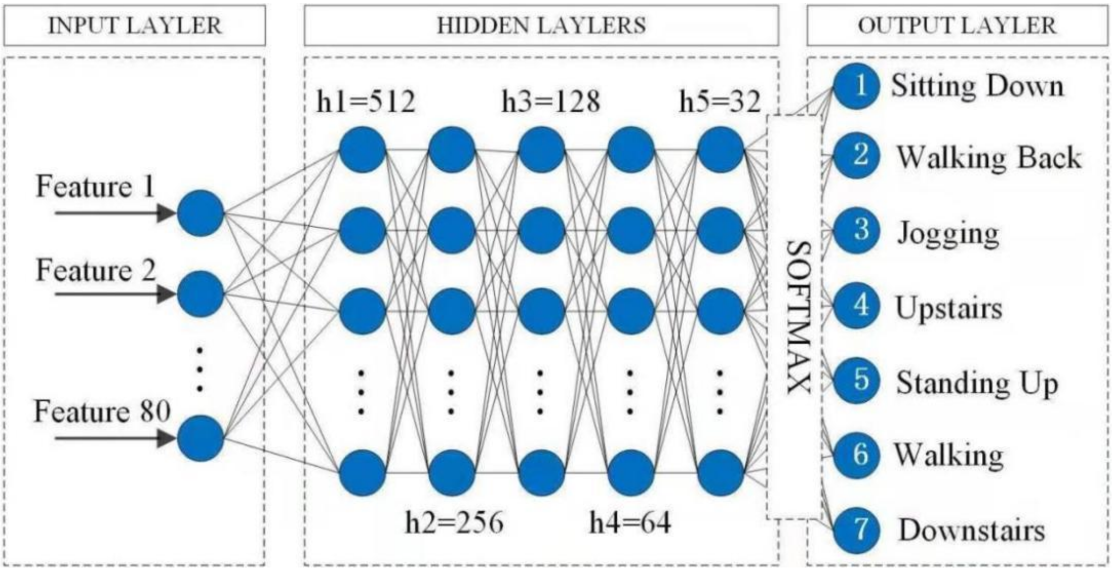

Figure 3. The architecture of the DNN.

2.4. Model Training and Evaluating

In this study, the dataset was divided into training and test sets, with a split rate of 4:1. Before feeding the data into the three models, random shuffling was implemented for this matrix. Next, the data were normalized by using the following normalization algorithm to avoid dilution of the effectiveness of lower-scale features in dealing with different-scale features:

$$v' = \frac{v - min(A)}{max(A) - min(A)} \tag{6}$$

where A is an input matrix, and v' and v are the new and old values of the matrix, respectively.

For the 1D-CNN and DNN, the weights with random values should be initialized in a normal distribution. In this study, the Adam optimizer was chosen to update the weights [27]. The training epoch, batch size, and learning rate were set as 2000, 800, and 0.001, respectively. The loss function was used to evaluate the model's performance in training. To minimize the loss, the gradient of the loss variation was back-propagated and used to update the weights. In our study, the categorical cross-entropy was selected to calculate the gap between the model output and the true label, which could be calculated by:

$$CE(x) = -\sum_{i=1}^{C} y_i \, log f_i(x) \tag{7}$$

where C denotes the categorical number (C equals 7 in our study), y is the expected output, and $f(x)$ is the model output and can be calculated by the activation function of x. Since the batch size samples are fed into the model, the average of the cross entropy is

$$CE(x)_{final} = \frac{\sum_{b=1}^{N} CE(x^b)}{N} \tag{8}$$

where N is the batch size and is set to 800.

3. Results

After finishing the feature extraction, the sEMG data were organized in a 4109 × 80 matrix (each row of the matrix was made up of 80 features). The dataset was divided into two parts: the training set and test set. To avoid uneven distribution of the test set, a five-fold cross-validation was applied in model training. The dataset was divided into training and test sets, with a split rate of 4:1. In our case, the training and test sets were 3288 × 80 and 821 × 80, respectively. For comparing the predicted results of lower limb motion recognition based on the 1D-CNN, DNN, and SVM models, both models were fed the same data, which had been preprocessed in the same way.

Figure 4 shows the confusion matrices of one fold in the five-fold cross-validation, which were the results of the recognition of seven daily motions based on the 1D-CNN, DNN, and SVM methods, respectively. Based on the confusion matrices, the precision, recall, F1-score, and accuracy were obtained (see Table 1). The results showed that the precision (1D-CNN: 97.5 ± 0.7; DNN: 95.5 ± 1.1; SVM: 93.8 ± 3.1, $P < 0.05$), recall (1D-CNN: 97.7 ± 0.9; DNN: 95.0 ± 3.5; SVM: 93.4 ± 2.9, $P < 0.05$), and F1-score (1D-CNN: 97.6 ± 0.6; DNN: 95.3 ± 2.2; SVM: 93.6 ± 2.2, $P < 0.05$) based on the 1D-CNN model were significantly higher than that based on the DNN and SVM model. Moreover, the accuracy of motion recognition based on our proposed 1D-CNN model improved to more than 97.7% and was higher than that based on the DNN and SVM model (95.5% and 93.7%, respectively).

Table 2 presents the precision, recall, F1-score, and accuracy of the five-fold cross-validation for recognition of all of the seven daily motions. Our proposed 1D-CNN model achieved consistent performance metrics, with a precision of 97.1 ± 0.6% (range: 96.5–98.0%), a recall of 96.9 ± 0.9% (range: 96.1–98.0%), a F1-score of 97.0 ± 0.8% (range: 96.3–98.0%), and an accuracy of 97.0 ± 0.8% (range: 96.3–98.1%). In addition, the precision, recall, F1-score, and accuracy of the five-fold cross-validation based on our proposed 1D-CNN model were all significantly improved compared with those based on DNN (precision: 95.0 ± 0.6%; recall: 94.6 ± 0.6%; F1-score: 94.8 ± 0.6%; accuracy: 95.0 ± 0.6%) and SVM (precision: 92.9 ± 0.7%; recall: 92.5 ± 0.8%; F1-score: 92.7 ± 0.7%; accuracy: 92.8 ± 0.7%) models ($P < 0.05$).

Moreover, the operating environment of all of the models was an Intel i7-10700 CPU @ 2.90 GHz, GTX-1660 GPU, and 16 GB RAM. To evaluate the real-time feasibility of the methods, the actual online computational costs were measured. The total preprocessing time, including single filtering, starting and ending detection, and feature extraction time, was 7.4 s. The model training time for 1D-CNN, DNN, and SVM was 4421 s, 2123 s, and 75 s, respectively. The model testing time for 1D-CNN, DNN, and SVM was 82 ms, 59 ms, and 0.4 ms, respectively.

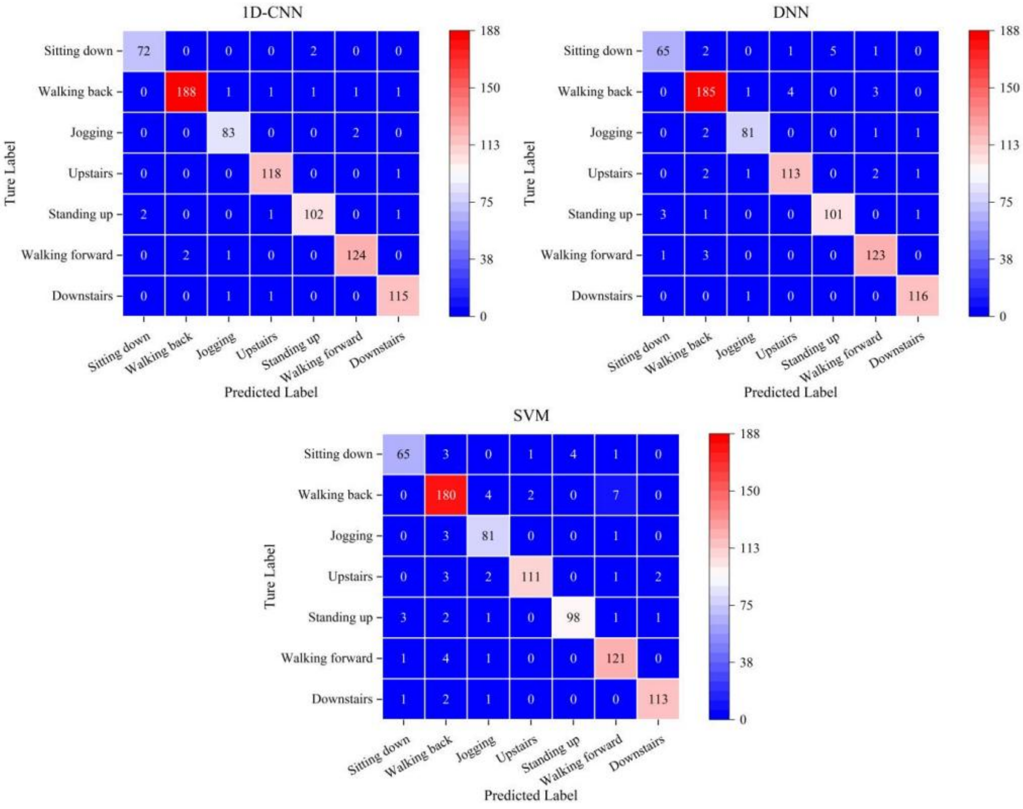

Figure 4. The confusion matrices for recognition of seven daily motions based on the 1D-CNN, DNN, and SVM models (one fold's results in the five-fold cross-validation; the training and test sets were 3288 × 80 and 821 × 80, respectively).

Table 1. Comparison of the precision, recall, F1-score, and accuracy of lower limb motion recognition based on the 1D-CNN, DNN, and SVM models (one fold's result in the five-fold cross-validation; the training and test sets were 3288 × 80 and 821 × 80, respectively).

		Sitting down	Walking back	Jogging	Going upstairs	Standing up	Walking forward	Going downstairs	Average ± SD
1D-CNN	Precision	97.3	98.9	96.5	97.5	97.1	97.6	97.5	97.5 ± 0.7
	Recall	97.3	97.4	97.6	99.2	96.2	97.6	98.3	97.7 ± 0.9
	F1-score	97.3	98.2	97.1	98.3	96.7	97.6	97.9	97.6 ± 0.6
	Accuracy	97.7							
DNN	Precision	94.2	94.9	96.4	95.8	95.3	94.6	97.5	95.5 ± 1.1
	Recall	87.8	95.9	95.3	95.0	95.3	96.9	99.1	95.0 ± 3.5
	F1-score	90.9	95.4	95.9	95.4	95.3	95.7	98.3	95.3 ± 2.2
	Accuracy	95.5							
SVM	Precision	92.9	91.4	90.0	97.4	96.1	91.7	97.4	93.8 ± 3.1
	Recall	87.8	93.3	95.3	93.3	92.5	95.3	96.6	93.4 ± 2.9
	F1-score	90.3	92.3	92.6	95.3	94.2	93.4	97.0	93.6 ± 2.2
	Accuracy	93.7							

Table 2. Comparison of the precision, recall, F1-score, and accuracy of lower limb motion recognition based on the 1D-CNN, DNN, and SVM models for the five-fold cross-validation.

	1D-CNN						DNN						SVM					
Fold	1	2	3	4	5	Mean ± SD	1	2	3	4	5	Mean ± SD	1	2	3	4	5	Mean ± SD
Precision	97.5	98.0	96.7	96.5	96.7	97.1 ± 0.6	95.5	95.4	94.6	94.1	95.4	95.0 ± 0.6	93.8	93.4	92.7	91.9	92.8	92.9 ± 0.7
Recall	97.7	98.0	96.3	96.1	96.4	96.9 ± 0.9	95.0	95.2	94.1	93.8	94.9	94.6 ± 0.6	93.4	93.1	92.2	91.5	92.3	92.5 ± 0.8
F1-score	97.6	98.0	96.5	96.3	96.5	97.0 ± 0.8	95.3	95.3	94.3	94.0	95.1	94.8 ± 0.6	93.6	93.2	92.4	91.7	92.5	92.7 ± 0.7
Accuracy	97.7	98.1	96.5	96.3	96.6	97.0 ± 0.8	95.5	95.4	94.5	94.2	95.2	95.0 ± 0.6	93.7	93.4	92.6	91.8	92.6	92.8 ± 0.7

4. Discussion

A 1D-CNN model was proposed in this study to recognize seven daily motions based on the eight-channel sEMG signals obtained from the eight main muscles of the human lower limbs. The results show that the proposed 1D-CNN had higher motion recognition accuracy than the traditional SVM and DNN models.

Compared with the DNN and SVM models, the proposed 1D-CNN model can significantly enhance the nonlinearity of neural networks, and then learn more complex functions like the transformation from sEMG signals to lower limb motions. Thus, the motion recognition accuracy based on the proposed 1D-CNN model was higher than that based on the DNN and SVM models. However, because of the more complex model structure and increased model parameters, the training time of 1D-CNN was longer than that of the DNN and SVM models. Through the convolutional and pooling operations, the 1D-CNN model can represent the local characteristics. In our study, three convolutional layers and three pooling layers were constructed in our proposed 1D-CNN model. The more convolutional layer and pooling layers, the higher the accuracy of motion recognition and the longer the training time of the neural network. Therefore, the accuracy and time consumption should be weighed on a case-by-case basis.

In this study, the TKEO method was applied for the detection of the starting and ending points of the sEMG signals. Delayed or early detection of muscle activation may lead to misclassification of movements. Due to the small amount of computation and ease of implementation, the TKEO method is suitable for the detection of the starting and ending points of the sEMG signals. The MAV and RMS were extracted as features to input into the proposed model. We all know that the more features extracted, the higher the accuracy of motion recognition. However, an increase in the number of features leads to an increase in the amount of computation and the input dimensions of the model. A compromise must be made between computation and accuracy.

At present, there are some studies that have classified more than three lower limb motions based on sEMG signals from lower limb muscles. Zhou et al. [9] classified four lower limb motions, including walking, going upstairs, going downstairs, and squatting, using a CNN–Transformer–LSTM (CNN-TL) fusion model, achieving an accuracy of 96.13%. Shi et al. [10] employed a scale unscented Kalman neural network to recognize five lower limb motions, including walking, crossing obstacles, standing up, going upstairs, and going downstairs, with an accuracy of 93.7%. Gautam et al. [28] applied a long-term recurrent convolution network (LRCN) to classify three lower limb motions, including walking, sitting down, and standing up, achieving an accuracy of 98.1%. Tu et al. [18] utilized an improved SVM model to distinguish three lower limb motions, including walking, standing, and sitting, with an accuracy of 96.03%. Furthermore, some studies have combined sEMG signal with accelerometer signals to classify lower limb motions. Hao et al. [29] recognized five lower limb motions, including walking, going upstairs, going downstairs, walking upslope, and walking downslope, based on combining sEMG and three-axis acceleration signals, using a two-stream hidden Markov model. The accuracy of motion recognition in their study was 94.3%. Ai et al. [30] classified five lower limb motions, including walking, going upstairs, going downstairs, standing, and squatting based on the sEMG and accelerometer signals. Based on the SVM model, the accuracy of motion recognition achieved was 98.1%. Compared with the above studies, our study employed the sEMG signal as the sole signal to classify up to seven lower limb motions, with our proposed 1D-CNN model achieving an exceptional classification accuracy of 97.0 ± 0.8%.

A number of limitations associated with this study are worth discussing. Firstly, the SNR of the sEMG signal is relatively low for the current sEMG acquisition devices. With the development of acquisition devices, the motion recognition accuracy of the proposed model can be further improved. Secondly, only three healthy men were recruited in this study. In order to further improve the generalization performance, larger cross-subject experiments will be conducted in our next work. Thirdly, a high window overlap (75%) was adopted in this study. Although high window overlap may introduce local similarity between adjacent samples, our classification accuracy demonstrates that the retained dynamic features outweigh any potential redundancy. In future work, we will further optimize the window parameters for specific motion types. Finally, only seven daily motions, i.e., walking forward, walking back, jogging, going upstairs, gping downstairs, standing up, and sitting down, were selected in our study. More daily motions, e.g., squatting, walking uphill, walking downhill, etc., will be used for motion recognition in the future.

The purpose of sEMG-based lower limb motion recognition is to achieve accurate control of an exoskeleton. Our next work will be focused on the application of the proposed method to the control of an exoskeleton. The research results and proposed model of this study are significant for research into exoskeleton control based on sEMG signals.

5. Conclusion

In this study, we proposed a 1D-CNN model to recognize seven daily motions, i.e., walking forward, walking back, jogging, sitting down, standing up, going upstairs, and going downstairs, based on the sEMG signals obtained from eight lower limb muscles, i.e, rectus femoris, vastus medial, vastus lateralis, biceps femoris, gastrocnemius medial, gastrocnemius lateralis, soleus, and tibialis anterior. The proposed model architecture mainly consisted of three 1D convolutional layers, three max-pooling layers, and one global average pooling layer. The TKEO method was applied for the detection of the starting and ending points of the sEMG signals. The MAV and RMS were extracted as the features to input into the proposed model. The results showed that the proposed 1D-CNN had higher motion recognition accuracy (97.0 ± 0.8%) than the DNN (95.0 ± 0.6%) and SNM (92.8 ± 0.7%) models. This study has significant implications for research into exoskeleton control based on sEMG signals.

Acknowledgments

This research is supported by the Shaanxi Province Postdoctoral Science Foundation (2023BSHGZZHQYXMZZ05).

Conflict of interest

The authors declare no conflicts of interest.

References

1. Sun J, Wang Y, Hou J, et al. (2024) Deep learning for electromyographic lower-limb motion signal classification using residual learning. *IEEE Trans Neural Syst Rehabil Eng* 32: 2078–2086. https://doi.org/10.1109/TNSRE.2024.3403723
2. Wang E, Chen X, Li Y, et al. (2024) Lower limb motion intent recognition based on sensor fusion and fuzzy multitask learning. *IEEE Trans Fuzzy Syst* 32: 2903–2914. https://doi.org/10.1109/TFUZZ.2024.3364382
3. Sun B, Cheng G, Dai Q, et al. (2021) Human motion intention recognition based on EMG signal and angle signal. *Cogn Comput Syst* 3: 37–47. https://doi.org/10.1049/ccs2.12002
4. Zhang L, Liu G, Han B, et al. (2020) Assistive devices of human knee joint: a review. *Robot Auton syst* 125: 103394. https://doi.org/10.1016/j.robot.2019.103394
5. Zhang LF, Ma Y, Wang C, et al. (2019) A method for arm motions classification and a lower-limb exoskeleton control based on sEMG singles. *IEEE Int Conf Adv Robot Mechatron* 2019: 118–123. https://doi.org/10.1109/ICARM.2019.8833708
6. Asai K, Takase N (2017) Finger motion estimation based on frequency conversion of EMG signals and image recognition using convolutional neural network. *IEEE Int Conf Control Autom Syst* 2017: 1366–1371. https://doi.org/10.23919/ICCAS.2017.8204206

7. Crepin R, Fall CL, Mascret Q, et al. (2018) Real-time hand motion recognition using sEMG patterns classification. *Annu Int Conf IEEE Eng Med Biol Soc* 2018: 2655–2658. https://doi.org/10.1109/EMBC.2018.8512820
8. Zhao DW, Ye XM, Wang S, et al. (2025) Upper limb human-exoskeleton system motion state classification based on semg: application of CNN-BiLSTM-attention model. *Sci Rep* 15: 18969. https://doi.org/10.1038/s41598-025-02864-5
9. Zhou ZW, Tao Q, Su N, et al. (2024) Lower limb motion recognition based on sEMG and CNN-TL fusion model. *Sensors* 24: 7087. https://doi.org/10.3390/s24217087
10. Shi X, Qin PJ, Zhu JQ, et al. (2020) Feature extraction and classification of lower limb motion based on sEMG signals. *IEEE Access* 8: 132882–1132892. https://doi.org/10.1109/ACCESS.2020.3008901
11. Zhang L, Yan Y, Liu G, et al. (2022) Effect of fatigue on kinematics, kinetics and muscle activities of lower limbs during gait. *Proc Inst Mech Eng H* 236: 1365–1374. https://doi.org/10.1177/09544119221112516
12. Liu G, Zhang L, Han B, et al. (2019) sEMG-based continuous estimation of knee joint angle using deep learning with convolutional neural network. *IEEE Int Conf Autom Sci Eng* 1: 140-145. https://doi.org/10.1109/COASE.2019.8843168
13. Kaiser JF (1990) On a simple algorithm to calculate the 'energy' of a signal. *Int Conf Acoust Speech Signal Process* 1: 381–384. https://doi.org/10.1109/ICASSP.1990.115702
14. Li X, Aruin A (2005) Muscle activity onset time detection using teager-kaiser energy operator. *Int Conf Eng Med Biol Soc* 7: 7549–7552. https://doi.org/10.1109/iembs.2005.1616259
15. Gu S, Yue Y, Maple C, et al. (2012) Classification of multi-channels SEMG signals using wavelet and neural networks on assistive robot. *Int Conf Ind Inform* 2012: 1158–1163. https://doi.org/10.1109/INDIN.2012.6301140
16. Chowdhury RH, Reaz MBI, Ali MABM, et al. (2013) Surface electromyography signal processing and classification techniques. *Sensors* 13: 12431–12466. https://doi.org/10.3390/s130912431
17. Chang Y, Wang L, Li M, et al. (2023) Research on gait recognition of surface EMG signal based on MPSO-LSTM algorithm. *J Mech Med Biol* 23: 2340066. https://doi.org/10.1142/S0219519423400663
18. Tu P, Li J, Wang H (2024) Lower limb motion recognition with improved SVM based on surface electromyography. *Sensors* 24: 3097. https://doi.org/10.3390/s24103097
19. Pourmokhtari M, Beigzadeh B (2024) Simple recognition of hand gestures using single-channel EMG signals. *Proc Inst Mech Eng H* 238: 372–380. https://doi.org/10.1177/09544119231225528
20. Shi X, Qin P, Zhu J, et al. (2020) Lower limb motion recognition method based on improved wavelet packet transform and unscented kalman neural network. *Math Probl Eng* 2020: 5684812. https://doi.org/10.1155/2020/5684812
21. Zhang W, Bai Z, Yan P, et al. (2024) Recognition of human lower limb motion and muscle fatigue status using a wearable FES-sEMG system. *Sensors* 24: 2377. https://doi.org/10.3390/s24072377
22. Solnik S, Rider P, Steinweg K, et al. (2010) Teager-Kaiser energy operator signal conditioning improves EMG onset detection. *Eur J Appl Physiol* 110: 489–498. https://doi.org/10.1007/s00421-010-1521-8
23. Hudgins B, Parker P, Scott RN (1993) A new strategy for multifunction myoelectric control. *IEEE Trans Biomed Eng* 40: 82–94. https://doi.org/10.1109/10.204774

24. Englehart K, Hudgins B (2003) A robust, real-time control scheme for multifunction myoelectric control. *IEEE Trans Biomed Eng* 50: 848–854. https://doi.org/10.1109/TBME.2003.813539
25. Ullah A, Ali S, Khan I, et al. (2020) Effect of analysis window and feature selection on classification of hand movements using EMG single. *Proc 2020 Intell Syst Conf* 3: 400–415. https://doi.org/10.1007/978-3-030-55190-2_30
26. Lin M, Chen Q, Yan S (2013) Network in network. *CoRR* abs/1312.4400: 1–10. https://arxiv.org/pdf/1312.4400
27. Kingma DP, Ba J. (2014) Adam: A method for stochastic optimization. *CoRR* abs/1412.6980: 1–15. https://arxiv.org/pdf/1412.6980
28. Gautam A, Panwar M, Biswas D, et al. (2020) MyoNet: a transfer-learning-based LRCN for lower limb movement recognition and knee joint angle prediction for remote monitoring of rehabilitation progress from sEMG. *IEEE J Transl Eng Health Med* 8: 1–10. https://doi.org/10.1109/JTEHM.2020.2972523
29. Hao J, Yang P, Chen L, et al. (2019) A gait patterns recognition approach based on surface electromyography and three-axis acceleration signals. *IOP Conf Ser Mater Sci Eng* 533: 012060. http://doi.org/10.1088/1757-899X/533/1/012060
30. Ai Q, Zhang Y, Qi W, et al. (2017) Research on lower limb motion recognition based on fusion of sEMG and accelerometer signals. *Symmetry* 9: 147. https://doi.org/10.3390/sym9080147